THE UNIVERSITY of EDINBURGH

Edinburgh Research Explorer

Nanosecond pulse width dependence of nonphotochemical laser-induced nucleation of potassium chloride

OPEN ACCESS

Nanosecond pulse-width dependence of nonphotochemical laser-induced nucleation of potassium chloride**

Martin R. Ward,[1] Iain Ballingall,[2] Matthew L. Costen,[2] Kenneth G. McKendrick[2]
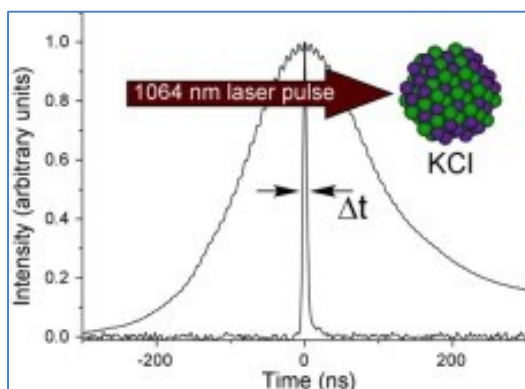and Andrew J. Alexander,[1,*]

[1] School of Chemistry, Joseph Black Building, University of Edinburgh, West Mains Road, Edinburgh, EH9 3JJ, UK.

[2] School of Engineering and Physical Sciences, Heriot-Watt University, Edinburgh, Scotland, United Kingdom, EH14 4AS.

[*]Corresponding author; e-mail: andrew.alexander@ed.ac.uk, Tel: +44-131-6504741, Fax: +44-131-6504743

Graphical abstract:

Abstract

The effect of laser pulse-width on the efficiency of nonphotochemical laser-induced nucleation (NPLIN) of supersaturated aqueous solutions of KCl has been studied. At equivalent peak power densities it was observed that the same fractions of samples were nucleated for both short (6 ns) and long (200 ns) near-infrared laser pulses. The results show that the efficiency depends on the peak power density and not on the duration, or total energy, of the laser pulses. It is concluded that the mechanism is unlikely to be based solely on diffusion of solute to a sub-critical cluster.

1. Introduction

Nonphotochemical laser-induced nucleation (NPLIN) of urea from supersaturated aqueous solution was discovered by Garetz et al. in 1996 [1]. They demonstrated that a train of nanosecond pulses (20 ns pulse width, ~0.1 J pulse^{-1}) of near-infrared light (1064 nm) from a laser could cause rapid crystallization from solution, and noted that the initially formed crystallites of urea were aligned preferentially along the direction of linear polarization of the electric-field of the laser light. They subsequently demonstrated the effect for other molecules, in particular for glycine which was also shown to crystallize into the α- or γ-glycine polymorphs depending on the polarization of the laser light [2,3]. Garetz et al. described a mechanism for NPLIN in terms of the optical Kerr effect: the high electric field strengths generated during the laser pulse can interact with the polarizability anisotropy of the molecules, and the interaction energy depends on the alignment of the molecules. Since the interaction energy between the light and a single molecule would be small (only ~10^{-4} $k_{B}T$ for glycine), it is believed that the light acts co-operatively on a cluster of molecules [3]. Garetz et al. observed that for the NPLIN to be effective, they required significant periods (hours, or days) of ageing of the supersaturated solutions prior to being shot with the laser. This is consistent with a requirement for growth and equilibration of pre-nucleating clusters in solution. The significance of pre-nucleating clusters to crystal nucleation in solution has become a hot topic for debate [4,5]. Studying the dynamics of the nucleation process by computer simulations is very challenging, since nucleation is a rare and random event [6]: recent simulations, however, have revealed the formation of liquid-like clusters of solute [5,7]. The postulated Kerr-effect mechanism for NPLIN fits in well with the concept of non-crystalline pre-nucleating clusters: molecules within the cluster are caused to align with the field, restructuring the cluster and lowering the free-energy barrier to nucleation. Recently, Alexander and Camp have demonstrated nucleation of potassium chloride (KCl) from supersaturated solutions by NPLIN with 1064 nm light, obtaining single crystals with a single laser pulse [8,9]. They observed no dependence of the nucleation probability on the polarization (circular or linear) of the light. Since KCl has no molecules to be aligned in the manner envisaged in the Kerr-effect mechanism, an alternative mechanism based on the *isotropic* polarizability of pre-nucleating clusters

of KCl was proposed. Their results were analyzed quantitatively using a theoretical model based on classical nucleation theory, and they reported a value for the crystal–solution interfacial tension of $\gamma = 2.19 \, \text{mJ m}^{-2}$.

In the studies of NPLIN reported thus far, the experimental data were reported as functions of the peak power of the laser pulse, since this corresponds to the peak of the electric field during the time that the radiation is present. Garetz et al. reported a threshold for NPLIN of urea corresponding to a peak power density of 30 MW cm^{-2} (9 ns pulses of 1064 nm light with linear polarization) [10]. By contrast, much higher powers 240–700 MW cm^{-2} were required to nucleate supersaturated solutions of glycine and histidine [11,12]. Myerson and co-workers have also used both nanosecond (4 ns pulses, 10 MW cm^{-2}) and picosecond (100 ps pulses, 220 MW cm^{-2}) laser pulses to nucleate hen egg-white lysozyme, although no quantitative analysis of the efficacy of peak power versus pulse width was reported [13]. Alexander and Camp measured threshold power densities of 6.4 MW cm^{-2} (7 ns pulses, 1064 nm) to nucleate solutions of KCl with a single laser pulse [8]. There have been other studies that have used femtosecond laser pulses to induce crystallization, for example, in anthracene and at surfaces of pre-existing urea crystals [14,15]. However, we note that the peak powers of the focussed light for these studies were significantly higher (~GW cm^{-2}), and the growth of crystals were ascribed to photomechanical processes, such as cavitation of the solution and ablation of crystalline surfaces causing secondary nucleation.

In this letter, we investigate the supposition that NPLIN depends on peak laser power density, and report the results of a study into the effect of the pulse width in the 6–200 nanosecond range on the efficiency of NPLIN of KCl from supersaturated solutions at 2 different solution concentrations. We confirm that the probability of nucleation is directly proportional to peak power density. The consequences of our results for possible microscopic mechanisms of NPLIN of KCl are discussed briefly.

2. Experimental

Supersaturated solutions were made by dissolving KCl (Fluka, puriss > 99%) in deionized water (Fisher, HPLC grade). The saturation concentration of KCl in aqueous solution at 24.4 °C ($c_S^{24.4}$) is 35.37 g per 100 g of H$_2$O. Two batches of solution were made, with supersaturations ($S = c / c_S^{24.4}$) of $S = 1.066$ and 1.076. These solutions were dissolved and filtered while hot through syringe filters (Minisart, 200 nm) into screw-cap glass vials (nominal diameter 20.3 mm). The volume of solution in

each vial was approximately 3.8 cm^3, and approximately 30 vials at each concentration were obtained. Once sealed, the vials can be reheated to dissolve any crystals.

Two separate Nd^{3+}:YAG laser systems were used to produce the short and long nanosecond pulses of near-infrared light (1064 nm). The short pulse was produced by the Q-switched output of a Nd^{3+}:YAG laser (Brilliant, Quantel, France). The long pulse was obtained from free running (i.e., non Q-switched) output of a Nd^{3+}:YAG laser (Spectron Laser, UK). The time dependences of the relative intensity of the pulses were measured using a fast photodiode (DET10A, Thorlabs, UK) with signals captured using a fast (1 GHz) digital-storage oscilloscope, giving a combined rise time ~1 ns. The spatial modes of the laser beams were nearly Gaussian (TEM00), and we verified that there were no hot spots in the beam, which was not focussed prior to entering the sample vial.

Each sample vial was intentionally set to crystallize and left overnight in order to ensure that all samples were treated equally. The solutions were dissolved by heating on a hotplate at 50 °C and each vial was shaken regularly: the heating and dissolution procedure took approximately 1 hour. Once the solutions were apparently dissolved, they were left to cool to 24.4 °C, and were left at this temperature for 30 minutes. It was found that one or two samples spontaneously nucleated during this time, probably due to having not been dissolved completely. We have observed that samples that do not nucleate within 30 minutes are normally stable for several days. Each sample vial was placed in the beam path and exposed to laser pulses for 10 s at a repetition rate of 10 Hz, giving a total of 100 shots for each sample. Having been shot, the samples were maintained at 24.4 °C. After about 15 minutes, some samples showed the presence of 1 or more crystals in the bottom of the vial. The number of sample vials that had nucleated in this sense was counted, and the fraction of the number of samples showing crystals (*n*) to the total number shot (*N*) was calculated as $p = \mathrm{n}/N$, with standard deviation estimated from the binomial distribution as $\sigma = \sqrt{p(1-p)/N}$.

3. Results and Discussion

3.1 Fraction of samples nucleated

Figure 1 shows a plot of typical pulses from each laser. The long pulse has a full-width at half-maximum (FWHM) of 200 ns, and the short pulse has a FWHM of 6 ns. The long pulse shows a broad envelope with a minor oscillation that is due to coherence between different electromagnetic modes of the light built-up in the laser cavity. We observed that the long pulse had a low-intensity tail that extends to long times ~20 μs. This tail was fitted and taken into account when determining the ratio of peak-power density to integrated power, as discussed below.
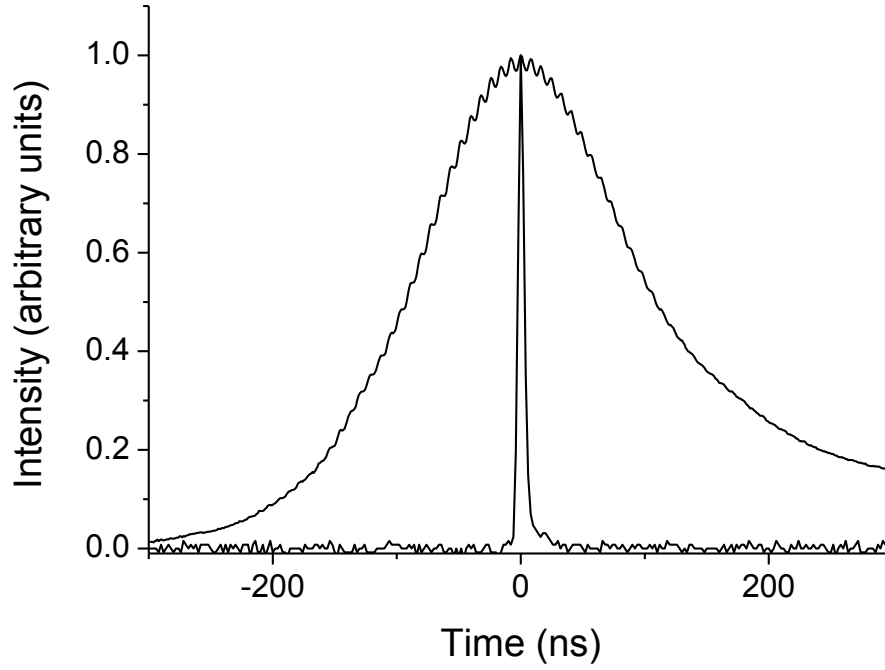
Figure 1. Time-dependent relative intensity of the laser pulses as measured using a fast photodiode. The relative intensity for each peak has been scaled to unity. The long pulse (free-running laser) has a full-width at half-maximum (FWHM) of 200 ns, the short pulse (Q-switched laser) has a FWHM of 6 ns.

The mean powers $\langle P \rangle$ of the light for both lasers running at 10 Hz were measured using a power meter. The mean pulse energy $\langle E \rangle$ is given by $\langle E \rangle = \langle P \rangle /(10\ \mathrm{s}^{-1})$. From the mean power, and knowing the time-dependence of the relative intensity as measured by photodiode, the peak power for each laser can be determined. From the traces in Fig. 1 we calculate a characteristic time factor T for each laser,

$$T = \frac{I_{\mathrm{peak}}}{I_{\mathrm{int}}},\qquad\qquad (1)$$

where I_{peak} is the relative peak intensity and I_{int} is the integrated area of the peak, as shown in Fig. 1. For the long pulse (free running) laser we find $T = 705$ ns, and for the short pulse (Q-switched) laser we obtain $T = 6.39$ ns. The peak power density can be obtained by calculating the effect of the slight focussing of the beam inside the sample vial using a simple optical ray-tracing procedure. The radius (r_0) of the beam for both lasers just before the sample vial was selected using an iris to be $r_0 =$

2.75 mm. We calculate the area of the laser pulse at the exit of the vial to be $A = 0.111$ cm^2. The mean peak power density $\langle j_{\text{peak}} \rangle$ is then obtained as

$$\langle j_{\text{peak}} \rangle = \frac{\langle P \rangle}{fA} \, . \quad (2)$$

This power density represents the average of the 100 shots used to irradiate each sample vial, and we will refer to it simply as the peak power density. We observed that fluctuations in the intensities of laser pulses for both lasers, as estimated from the photodiode, were < 5 %.

The maximum power for the experiments was limited by the power output of the free-running laser, which was operated at its maximum flashlamp voltages. The samples at $S = 1.076$ were shot at a slightly higher mean power $\langle P \rangle = 1.80$ W than those at $S = 1.066$, which were shot at $\langle P \rangle = 1.67$ W. For each set of samples, from the peak power density of the free-running laser, we calculated the mean pulse energy required from the Q-switched laser so that the peak power densities of both laser pulses would be approximately the same. The beam of the Q-switched laser was passed through a high power-Glan laser polarizer (Optics for Research, NJ, USA) which, by rotation relative to the natural linear polarization of the laser output, was used to control the pulse power before entering the sample vial.

Supersaturation of samples (S)	Laser operation	Pulse width / ns	Mean power $\langle P \rangle$ / W	Mean pulse energy $\langle E \rangle$ / mJ pulse^{-1}	Peak power density $\langle j_{\text{peak}} \rangle$ / MW cm^{-2}	Fraction of samples nucleated (p/N)
1.066	free running	202	1.67	167	2.14	0.21 ± 0.08
	Q switched	6	0.0155	1.55	2.19	0.24 ± 0.08
1.076	free running	202	1.80	180	2.30	0.31 ± 0.08
	Q switched	6	0.0160	1.60	2.26	0.26 ± 0.08

Table 1. Characteristics of the laser pulses used to nucleate KCl solutions, and the fraction of samples nucleated. The mean power of pulses from the Q-switched laser was selected by means of a near-infrared polarizer in order to obtain similar peak power densities as for the free-running laser for each sample set.

In previous work, we demonstrated that the probability of nucleation of supersaturated aqueous KCl solutions is linearly proportional to the peak power density [9]. In the present work we have chosen conditions such that the peak power density is nearly the same for each of the laser pulses. The details of the laser pulses used and the resulting fraction of samples nucleated are shown in Table 1. As can be seen from the table, the fractions of samples nucleated by each laser are approximately equal for a given saturation: thus, for $S = 1.076$, the fraction of samples nucleated is $p \sim 0.29$ and for $S = 1.066$, $p \sim 0.23$. However, the mean energy being delivered to the samples differs between lasers by more than 2 orders of magnitude: e.g., for $S = 1.076$, the mean energy per pulse was 180 mJ from the free-running laser and 1.60 mJ from the Q-switched laser.

We might expect absorption of some of the energy of the laser pulses by the solution to cause heating, thereby reducing the observed nucleation fraction. This effect would be greatest for the free-running laser, where the pulse energies are higher. The absorption coefficient of pure water has been reported as 0.1442 cm^{-1} at 1063 nm [16]. The absorption is not expected to be significantly different for a saturated solution of aqueous KCl, which we verified by near-infrared spectroscopy. If we take the pathlength to be the diameter of the vial (2 cm), then the energy absorbed per 180 mJ pulse will be 87.3 mJ. The specific heat capacity of KCl brine ($S = 0.985$, 298.15 K) was reported to be $c_p = 3005$ J g^{-1} K^{-1} [17,18]. To estimate the resulting temperature rise over 100 shots, we assume that free convection and conduction from the nearly cylindrical volume (0.35 cm^3) of solution irradiated takes place [19]. We estimate that the mean temperature rise within the irradiated volume of the solution using the Q-switched laser (1.6 mJ pulse^{-1}) would be 2 mK after 100 pulses, which is entirely negligible. The mean temperature rise over 100 pulses in the irradiated volume using the free-running laser would be 2.1 K, corresponding to a 1.8% decrease in supersaturation, which is not significant compared to the estimated statistical uncertainties quoted in Table 1. Our estimates do not take into account forced convection of the solution due to manual handling of the sample vials or heat loss to the surroundings, both of which would also work to offset effects of the temperature rise.

3.2 Estimate of critical cluster size

Our experimental results support the hypothesis that peak power and not the total energy of the laser pulse determines the NPLIN efficiency. The peak electric field (E_{peak}) of the light in absence of the solution can be calculated from the peak power density as [20]

$$E_{\text{peak}} = \sqrt{\frac{2\langle j_{\text{peak}} \rangle}{c\varepsilon_0}} \qquad (3)$$

where c is the speed of light and ε_0 is the permittivity of free space. Using Eq. (3) we calculate that peak fields for our experiments are in the range $E_{\text{peak}} = 4.02\text{–}4.16 \times 10^6$ V m^{-1}. Note that Eq. (3) is written for the free field (*in vacuo*) since this is the value to be used in the equations that follow. The actual peak electric field in the solution will be reduced by a factor $\sqrt{\varepsilon_{\text{aq}}} = n_{\text{aq}}$ where n_{aq} is the refractive index of the supersaturated solution. The free energy change $\Delta G(r, E)$ for formation of a spherical cluster of radius r in the presence of an applied electric field E can be written [8]

$$\Delta G(r, E) = 4\pi r^2 \gamma - \frac{4}{3}\pi r^3 \left(A \ln S + aE^2 \right) \qquad (4)$$

where γ is the solution–crystal interfacial tension, S is the supersaturation (as defined in Sec. 2), and E is the electric field (in vacuo, as calculated above). The parameter $A = \rho RT/M$, where ρ is the mass density and M is the molar mass of solid KCl. At 24.4 °C, we calculate $A = 6.584 \times 10^7$ J m^{-3}. The term aE^2 is the additional energy density of the particle due to the presence of the electric field, where a is written in terms of the relative dielectric constants of the particle, ε_p, and the aqueous solvent, ε_{aq} [21]:

$$a = \frac{3\varepsilon_0 \varepsilon_{aq}}{2} \left(\frac{\varepsilon_p - \varepsilon_{aq}}{\varepsilon_p + 2\varepsilon_{aq}} \right). \qquad (5)$$

For KCl in water, using tabulated refractive indices at 1064 nm [22], we obtain $a = 1.783 \times 10^{-12}$ F m^{-1}. Eq. (4) predicts a maximum in ΔG which occurs at a critical cluster radius $r = r_c(E)$ given by

$$r_c(E) = \frac{2\gamma}{A \ln S + aE^2}. \qquad (6)$$

At supersaturation $S = 1.066$, with a peak electric field of $E = 4.02 \times 10^6$ V m^{-1} and using $\gamma = 2.19$ mJ m^{-2} for the solution–crystal interfacial tension [8], we calculate a critical cluster size $r_c = 1$ nm, corresponding to an anhydrous cluster containing ~76 units of KCl.

3.3 Nucleation mechanism

The present results do not reveal a complete picture of the microscopic mechanism for NPLIN of KCl but they do bring us some vital clues. *Prima facie*, we might consider two viable microscopic mechanisms: (1) during the presence of the electric field, sufficient solute is attracted to a pre-existing cluster causing it to become large enough such that it remains critical after the field has gone; or, (2) the presence of the electric field stimulates a structural rearrangement of the KCl within a subcritical cluster: e.g., this might involve a transition from a liquid-like structure to one that is more crystalline.

For the mechanism based on solute transport (1), we consider the amount of solute that could be involved, considering the timescales involved. From experimental measurements of the diffusivity of supersaturated KCl [23], we calculate $D = 1.87 \times 10^{-9}$ m^2 s^{-1} at $S = 1.066$. From this diffusivity, we calculate the root-mean-square radius of diffusion,

$$r_{\mathrm{rms}} = \left\langle r^2 \right\rangle^{1/2} = \left(6Dt\right)^{1/2}, \qquad (7)$$

This means that solute within a radius of ~23 nm of the initial sub-critical cluster could be attracted during the 48 ns that the long pulse is at 95% of its peak intensity. From the density of a saturated solution of KCl (1.1778 g cm^{-3}) we calculate that there are 2.5 x 10^{27} m^{-3} KCl units in solution. Taken together, all of the solute within a radius of 23 nm in solution could potentially form a crystalline cluster of radius ~13 nm, i.e., beyond the critical radius even for large values of the solution–solute interfacial tension, γ [24].

However, from the shape of the long pulse in Fig. 1, we note that the full width at 95% peak intensity (48 ns) is 8 times the FWHM of the Q-switched pulse, and yet the fractions of nucleation are not significantly different under the conditions we have tested. It seems clear then, that the critical point can be reached in the time of the shorter pulse, and that there appears to be no significant advantage gained by the field being present for longer, as one might expect for a mechanism based on solute diffusion alone. We conclude that mechanism (2), involving some field-induced re-arrangement of the cluster, is the most likely based on the experimental evidence so far. Further theoretical and experimental work should be carried out to understand the microscopic mechanism.

5. Conclusions

We have studied the effects of nanosecond pulse width on the efficiency of nonphotochemical laser-induced nucleation (NPLIN) of aqueous solutions of potassium chloride. At equivalent peak power densities it was observed that the same fractions of samples were nucleated for both short (6 ns) and

long (200 ns) laser pulses. The results show that the efficiency of NPLIN depends on the peak power density of the laser pulse, and not on the total energy delivered to the solution. The critical cluster radius for NPLIN in the present experiments was estimated to be 1 nm. The results suggest that the microscopic mechanism for NPLIN of KCl in aqueous solution is unlikely to be based on diffusion of solute to a sub-critical cluster during the presence of the field, since it would be expected that much more solute could be transferred during the longer pulse. We conclude that field-induced rearrangement of a pre-nucleating cluster is the most likely mechanism for NPLIN at the present time.

References

[1] B. A. Garetz, J. E. Aber, N. L. Goddard, R. G. Young, A. S. Myerson: Nonphotochemical, polarization-dependent, laser-induced nucleation in supersaturated aqueous urea solutions. *Phys. Rev. Lett.* 77 (1996) **3475**.

[2] J. Zaccaro, J. Matic, A. S. Myerson, B. A. Garetz: Nonphotochemical, laser-induced nucleation of supersaturated aqueous glycine produces unexpected gamma-polymorph. *Cryst. Growth Des.* 1 (2001) **5**.

[3] B. A. Garetz, J. Matic, A. S. Myerson: Polarization switching of crystal structure in the nonphotochemical light-induced nucleation of supersaturated aqueous glycine solutions. *Phys. Rev. Lett*. 89 (2002) **175501**.

[4] D. Gebauer, A. Volkel, H. Colfen: Stable Prenucleation Calcium Carbonate Clusters. *Science* 322 (2008) **1819**.

[5] D. Zahn: Atomistic mechanism for NaCl nucleation from an aqueous solution. *Phys. Rev. Lett.* 92 (2004) **040801**.

[6] S. Auer, D. Frenkel: Prediction of absolute crystal-nucleation rate in hard-sphere colloids. *Nature* 409 (2001) 1020.

[7] J. Anwar, P. K. Boateng: Computer simulation of crystallization from solution. *J. Am. Chem. Soc.* 120 (1998) **9600**.

[8] C. Duffus, A. J. Alexander, P. J. Camp: Spatial Control of Crystal Nucleation in Agarose Gel. *J. Am. Chem. Soc.* 131 (2009) **11676**.

[9] A. J. Alexander, P. J. Camp: Single Pulse, Single Crystal Laser-Induced Nucleation of Potassium Chloride. *Crystal Growth Des.* 9 (2009) **958**.

[10] J. Matic, X. Y. Sun, B. A. Garetz, A. S. Myerson: Intensity, wavelength, and polarization dependence of nonphotochemical laser-induced nucleation in supersaturated aqueous urea solutions. *Cryst. Growth Des.* 5 (2005) **1565**.

[11] X. Sun, B. A. Garetz, A. S. Myerson: Supersaturation and polarization dependence of polymorph control in the nonphotochemical laser-induced nucleation (NPLIN) of aqueous glycine solutions. *Cryst. Growth Des.* 6 (2006) **684**.

[12] X. Sun, B. A. Garetz, A. S. Myerson: Polarization switching of crystal structure in the nonphotochemical laser-induced nucleation of supersaturated aqueous L-histidine. *Cryst. Growth Des.* 8 (2008) **1720**.

[13] I. S. Lee, J. M. B. Evans, D. Erdemir, A. Y. Lee, B. A. Garetz, A. S. Myerson: Nonphotochemical Laser Induced Nucleation of Hen Egg White Lysozyme Crystals. *Cryst. Growth Des.* 8 (2008) **4255**.

[14] H. Y. Yoshikawa, Y. Hosokawa, H. Masuhara: Explosive crystallization of urea triggered by focused femtosecond laser irradiation. Jap. *J. Appl. Phys.* 45 (2006) **L23**.

[15] K. Nakamura, Y. Hosokawa, H. Masuhara: Anthracene crystallization induced by single-shot femtosecond laser irradiation: Experimental evidence for the important role of bubbles. *Cryst. Growth Des.* 7 (2007) **885**.

[16] L. H. Kou, D. Labrie, P. Chylek: Refractive-Indexes of Water and Ice in the 0.65-Mu-M to 2.5-Mu-M Spectral Range. *Appl. Opt.* 32 (1993) **3531**.

[17] D. A. Fletcher, R. F. McMeeking, D. Parkin: The United Kingdom Chemical Database Service. *J. Chem. Inf. Comput. Sci.* 36 (1996) **746**.

[18] Y. A. Epikhin, M. S. Stakhanova, M. K. Karapetyants: Volume and heat capacity changes in aqueous salt solutions. IV. The potassium chloride - potassium iodide - water and potassium chloride - potassium fluoride - water systems. Russ. *J. Phys. Chem.* 40 (1966) **201**.

[19] R. B. Bird, W. E. Stewart, E. N. *Lightfoot: Transport Phenomena,* J. Wiley & Sons, NY, 1960.

[20] J. D. Jackson: *Classical Electrodynamics*, Wiley, New York, 1998.

[21] J. O. Isard: Calculation of the influence of an electric field on the free energy of formation of a nucleus. *Phil. Mag.* 35 (1977) **817**.

[22] Handbook of Chemistry and Physics in D.R. Lide (Ed.), *Handbook of Chemistry and Physics.* CRC Press, Boca Raton, FL, 2007.

[23] Y. C. Chang, A. S. Myerson: The diffusivity of potassium chloride and sodium chloride in concentrated, saturated, and supersaturated aqueous solutions. *AiChE Journal* 31 (1985) **890**.

[24] A. E. Nielsen, O. Söhnel: Interfacial Tensions Electrolyte Crystal-Aqueous Solution, from Nucleation Data. *J. Cryst. Growth* 11 (1971) **233**.